AIP | Journal of Applied Physics

Piezoelectric anisotropy of a KNbO3 single crystal

Linyun Liang, Y. L. Li, S. Y. Hu, Long-Qing Chen, and Guang-Hong Lu

Citation: J. Appl. Phys. **108**, 094111 (2010); doi: 10.1063/1.3511336

View online: http://dx.doi.org/10.1063/1.3511336

View Table of Contents: http://jap.aip.org/resource/1/JAPIAU/v108/i9

Published by the American Institute of Physics.

Piezoelectric anisotropy of a $KNbO_3$ single crystal

Linyun Liang,[1,3] Y. L. Li,[2] S. Y. Hu,[2] Long-Qing Chen,[3] and Guang-Hong Lu[1,a)]
[1]*Department of Physics, Beijing University of Aeronautics & Astronautics, Beijing 100191, China*
[2]*Pacific Northwest National Laboratory, Richland, Washington 99352, USA*
[3]*Department of Materials Science & Engineering, The Pennsylvania State University, Pennsylvania 16802, USA*

(Received 27 July 2010; accepted 2 October 2010; published online 11 November 2010)

Orientation dependence of the longitudinal piezoelectric coefficients (d_{33}^{*}) of a $KNbO_3$ single crystal has been investigated as a function of temperature by using the Landau–Ginzburg–Devonshire phenomenological theory. It is shown that the maximum of d_{33}^{*} is not always along the polarization direction of the ferroelectric phase. The enhancement of d_{33}^{*} along a nonpolar direction is attributed to a ferroelectric phase transition at which a polarization changes its direction. In the tetragonal phase, the maximum of d_{33}^{t*} at high temperatures is along the tetragonal polar direction and then changes its direction toward the polar direction of the orthorhombic phase when the temperature is close to the tetragonal-orthorhombic phase transition. The maximum of d_{33}^{o*} of the orthorhombic phase depends on both the high-temperature and low temperature ferroelectric phase transitions. In the rhombohedral phase, the maximum of d_{33}^{r*} is relatively insensitive to temperature due to the absence of any further phase transitions in the low temperature regime. These results can be generalized to the phase transitions induced by external electric field, pressure, and composition variations. © *2010 American Institute of Physics*. [doi:10.1063/1.3511336]

I. INTRODUCTION

Pb(Zr, Ti)O_3 (PZT) ceramics are widely used in actuator devices due to their excellent piezoelectric properties near the morphotropic phase boundary (MPB).[1,2] However, there has been increasing interest in lead-free materials due to environmental concerns. Candidate materials for lead-free piezoelectric ceramics include $BaTiO_3$, $(Bi_{0.5}Na_{0.5})TiO_3$, $(Bi_{0.5}K_{0.5})TiO_3$, $(Na_{0.5}K_{0.5})NbO_3$, and $KNbO_3$.[3–6] As a simple perovskite, $BaTiO_3$ has been intensively studied both in single crystal and ceramic forms for many years. However, much less is known about $KNbO_3$, for which the ferroelectricity was first observed about 60 years ago. The main reason may come from the difficulties of growing $KNbO_3$ single crystals and then poling a multidomain structure into single-domain at room temperature.[7] Furthermore, the high phase transition temperature between tetragonal and orthorhombic ferroelectric phases induces further complexity due to additional domain structure formation upon cooling. As a result, it is difficult to measure the temperature dependence of spontaneous polarization and the single domain dielectric properties at higher temperatures.

Recent discovery of exceptionally large piezoelectric responses along nonpolar directions in lead-based relaxor-ferroelectric solid solutions[8] has generated interest in simple perovskite ferroelectric materials such as $BaTiO_3$ and $KNbO_3$. These classic ferroelectric materials may display effects similar to complex solid solutions. The studies of simple structure materials can avoid complexities associated with mesoscopic structures of relaxor-ferroelectric solid solutions. For the tetragonal $BaTiO_3$ single crystal, a higher piezoelectric response was observed along no-polar $[111]^c$ directions, where the superscript "*c*" refers to the cubic phase.[9] While in the orthorhombic phase, the highest piezoelectric responses with d_{33} over 500 pC/N were observed when an electric field was applied along $[001]^c$ no-polar direction.[10] However, this excellent piezoelectric performance of monoclinic $BaTiO_3$ crystal cannot be used at room temperature since the monoclinic phase of $BaTiO_3$ is stable below 5 °C.

Due to a large piezoelectricity and a high Curie point,[11,12] $KNbO_3$ ceramics has been considered as one of the candidate materials for future lead-free piezoelectric applications. The electromechanical coupling factor of the thickness-extensional mode, k_t, in a $KNbO_3$ crystal reaches as high as 0.69 for the 49.58°-rotated *X*-cut about the *y*-axis, which is the highest among all current known piezoelectric materials.[11] Moreover, the predicted longitudinal piezoelectric coupling factor for the width-extensional mode, k_{11}', is as high as 82.4% for the 43.5° rotated *Z*-cut plate about the *y*-axis. This value is comparable to that of $Pb(Zn_{1/3}Nb_{2/3})O_3-PbTiO_3$.[13] Wiesendanger[14] measured d_{15} and d_{24} of $KNbO_3$ single-domain crystals by applying a resonance-antiresonance method. Gunter[15] measured d_{31}, d_{32}, and d_{33} of $KNbO_3$ single-domain crystals using the quasi-static method. Zgonik *et al.*[16] calculated the complete set of piezoelectric d_{ij} constants. Wada *et al.*[12] investigated the piezoelectric properties of $KNbO_3$ crystals along the polar $[110]^c$ direction and $[001]^c$ of engineered domain direction. Piezoelectric coefficient d_{31} along nonpolar $[001]^c$ direction was 2.8 times higher than that along the polar $[110]^c$ direction. It is noticed that all experiments were performed at room temperature and there are significant discrepancies among them. Furthermore, there is a lack of complete piezo-

a)Electronic mail: lgh@buaa.edu.cn.

electric coefficients for all three ferroelectric phases and their dependence on crystal orientation, temperature, electric field, and pressure.

The enhancement of piezoelectric coefficients was attributed to the polarization rotation under an external electric field, domain wall contributions in engineered domain structures,[17] and phase transitions induced by temperature or external field.[18] The piezoelectric response can be analyzed using the Landau–Ginzburg–Devonshire (LGD) phenomenological approach.[19,20] For example, the orientation dependences of longitudinal piezoelectric coefficient at various temperatures, stress, and composition were analyzed for $BaTiO_3$, $PbTiO_3$, and PZT materials.[6,21]

In this paper, we employ the LGD thermodynamic phenomenological theory to calculate and predict the piezoelectric coefficients in the three ferroelectric phases of $KNbO_3$ crystal under various temperatures and their orientation dependence of the longitudinal piezoelectric coefficient d_{33}^*. The enhancement in piezoelectric coefficients induced by temperature along polar and no-polar directions was discussed in term of polarization rotation and contraction, and the flattening of the free energy landscape near a phase transition.

II. PHENOMENOLOGICAL THEORY

In the framework of the LGD-type phenomenological theory, the free energy function is expanded as a polynomial of the components of polarization $\boldsymbol{P}=(P_1,P_2,P_3)$. An eighth-order polynomial is employed to describe the free energy of $KNbO_3$ single crystal since a six-order polynomial is not enough to describe the three phase transitions in the ferroelectric temperature regime unless we assume the high-order expansion coefficients depends on the temperature. Using the free energy of the paraelectric phase as a reference, the free energy of $KNbO_3$ single crystal can be expressed as

$$
\begin{aligned}
f_{\mathrm{LGD}}(P_1,P_2,P_3) = f_{\mathrm{chem}} + f_{\sigma} = {} & \alpha_1(P_1^2+P_2^2+P_3^2) + \alpha_{11}(P_1^4 \\
& + P_2^4+P_3^4) + \alpha_{111}(P_1^2P_2^2+P_2^2P_3^2 \\
& + P_1^2P_3^2) + \alpha_{111}(P_1^6+P_2^6+P_3^6) \\
& + \alpha_{112}[P_1^4(P_2^2+P_3^2)+P_2^4(P_1^2+P_3^2) \\
& + P_3^4(P_1^2+P_2^2)] + \alpha_{123}P_1^2P_2^2P_3^2 \\
& + \alpha_{1111}(P_1^8+P_2^8+P_3^8) + \alpha_{1112}[P_1^6(P_2^2 \\
& + P_3^2) + P_2^6(P_1^2+P_3^2) + P_3^6(P_1^2+P_2^2)] \\
& + \alpha_{1122}(P_1^4P_2^4+P_2^4P_3^4+P_1^4P_3^4) \\
& + \alpha_{1123}(P_1^4P_2^2P_3^2+P_2^4P_3^2P_1^2+P_3^4P_1^2P_2^2) \\
& - \frac{1}{2}s_{11}(\sigma_1^2+\sigma_2^2+\sigma_3^2) - s_{12}[\sigma_1\sigma_2 \\
& + \sigma_2\sigma_3+\sigma_3\sigma_1] - \frac{1}{2}s_{44}[\sigma_4^2+\sigma_5^2+\sigma_6^2] \\
& - Q_{11}[\sigma_1P_1^2+\sigma_2P_2^2+\sigma_3P_3^2] \\
& - Q_{12}[\sigma_1(P_2^2+P_3^2)+\sigma_2(P_1^2+P_3^2) \\
& + \sigma_3(P_1^2+P_2^2)] - Q_{44}[\sigma_4P_2P_3 \\
& + \sigma_5P_1P_3 + \sigma_6P_1P_2],
\end{aligned}
\tag{1}
$$

where α with subscript index represents energy expansion coefficient, σ_i is stress component, s_{ij} is elastic compliance at constant polarization, and Q_{ij} is the electrostrictive coupling coefficient between polarization and stress.

The dielectric stiffness coefficient χ_{ij} can be obtained via a second partial derivative of the free energy function as

$$\chi_{ij} = \varepsilon_0 \partial^2 f_{\mathrm{LGD}}/\partial P_i\,\partial P_j, \quad (i,j=1,2,3). \tag{2}$$

The dielectric susceptibility coefficients (η_{ij}) can be determined from the reciprocal of the dielectric stiffness (χ_{ij}) using the following relation,

$$\eta_{ij} = A_{ji}/\Delta, \quad (i,j=1,2,3), \tag{3}$$

where A_{ji} and Δ are the cofactor and determinant of the χ_{ij} matrix.

The piezoelectric coefficient g_{ij} representing the coupling between polarization and stress is derived from the following equation:

$$g_{ij} = -\partial^2 f_{\mathrm{LGD}}/\partial P_i\,\partial\sigma_j, \quad (i=1,2,3, \quad j=1,2,3,4,5,6). \tag{4}$$

The piezoelectric coefficients d_{ij} representing the coupling between polarization and strain can be calculated by

$$d_{ij} = \varepsilon_0 \eta_{ik} g_{kj}, \quad (k=1,2,3). \tag{5}$$

It is convenient to write piezoelectric coefficients in the cubic crystallographic coordinate system. We use a superscript c to indicate the cubic crystallographic coordinate system. The piezoelectric coefficients for the three ferroelectric phases in the cubic crystallographic coordinate system have the following forms:[22]

For the tetragonal phase with $P_1=P_2=0$, $P_3=P_{3T}^c\neq 0$,

$$
\begin{aligned}
& d_{33T}^c = 2\varepsilon_0\eta_{33T}^c Q_{11}P_{3T}^c, \\
& d_{31T}^c = d_{32T}^c = 2\varepsilon_0\eta_{33T}^c Q_{12}P_{3T}^c, \\
& d_{15T}^c = d_{24T}^c = \varepsilon_0\eta_{11}^c Q_{44}P_{3T}^c, \\
& d_{11T}^c = d_{12T}^c = d_{13T}^c = d_{14T}^c = d_{16T}^c = 0, \\
& d_{21T}^c = d_{22T}^c = d_{23T}^c = d_{25T}^c = d_{26T}^c = d_{34T}^c = d_{35T}^c = d_{36T}^c = 0.
\end{aligned}
\tag{6}
$$

For the orthorhombic phase with $P_1=0$, $P_2=P_3=P_{3O}^c\neq 0$,

$$
\begin{aligned}
& d_{15O}^c = d_{16O}^c = \varepsilon_0\eta_{11O}^c Q_{44}P_{3O}^c, \\
& d_{24O}^c = d_{34O}^c = \varepsilon_0(\eta_{33O}^c + \eta_{32O}^c)Q_{44}P_{3O}^c, \\
& d_{31O}^c = d_{21O}^c = 2\varepsilon_0(\eta_{32O}^c + \eta_{33O}^c)Q_{12}P_{3O}^c, \\
& d_{32O}^c = d_{23O}^c = 2\varepsilon_0(Q_{11}\eta_{32O}^c + Q_{12}\eta_{33O}^c)P_{3O}^c, \\
& d_{33O}^c = d_{22O}^c = 2\varepsilon_0(Q_{12}\eta_{32O}^c + Q_{11}\eta_{33O}^c)P_{3O}^c,
\end{aligned}
$$

$$d^c_{11O}=d^c_{12O}=d^c_{13O}=d^c_{14O}=d^c_{25O}=d^c_{26O}=d^c_{35O}=d^c_{36O}=0. \tag{7}$$

For the rhombohedral phase with $P_1=P_2=P_3=P^c_{3R}\neq 0$,

$$d^c_{11R}=d^c_{22R}=d^c_{33R}=2\varepsilon_0(\eta^c_{11R}Q_{11}P^c_{3R}+2\eta^c_{12}Q_{12}P^c_{3R}),$$

$$d^c_{12R}=d^c_{13R}=d^c_{21R}=d^c_{23R}=d^c_{31R}=d^c_{32R}=2\varepsilon_0(\eta^c_{11R}Q_{12}P^c_{3R}+\eta^c_{12R}(Q_{11}+Q_{12})P^c_{3R}),$$

$$d^c_{15R}=d^c_{16R}=d^c_{24R}=d^c_{26R}=d^c_{34R}=d^c_{35R}=\varepsilon_0(\eta^c_{11R}+\eta^c_{12R})Q_{44}P^c_{3R},$$

$$d^c_{14R}=d^c_{25R}=d^c_{36R}=2\varepsilon_0\eta^c_{12R}Q_{44}P^c_{3R}. \tag{8}$$

The subscripts $P=T,O,R$ of the dielectric susceptibility η^c_{ijP}, polarization P^c_{iP}, and piezoelectric coefficient d^c_{ijP} represent the tetragonal, orthorhombic, and rhombohedral phases, respectively. The superscript index c indicates that physical quantities are measured in the cubic crystallographic coordinate system.

In the foregoing, the Voigt's notation of the piezoelectric coefficient $d_{ij}(i=1,2,3;\ j=1,2,3,4,5,6)$ is used. But its tensor notation $d_{ijk}(i,j,k=1,2,3)$ has to be employed for coordinate transformation. Their relation between the Voigt's notation and tensor notation is $d_{im}=d_{ijk}$ $(m=j=k=1,2,3)$ and $d_{im}=2d_{ijk}$ $(j\neq k,\ m=9-j-k,\ m=4,5,6)$.

The piezoelectric coefficients, d^p_{ijk}, in the new coordinate that is associated with one of the three ferroelectric phases can be obtained by the transformation from the cubic crystallographic coordinate system d^c_{lmn} as[23]

$$d^p_{ijk}=c_{il}c_{jm}c_{kn}d^c_{lmn}, \tag{9}$$

where c_{ij} is the element of the transformation matrix that describes the rotation from the original cubic coordinate system to the new coordinate system notated by the superscript "p" with $p=t,o,r$, representing the coordinate system associated with the tetragonal, orthorhombic, and rhombohedral phases, respectively.

If a further rotation is made with respect to the ferroelectric phase coordinate, the piezoelectric coefficient d^{p*}_{ijk} defined in the rotated coordinate can be calculated by

$$d^{p*}_{ijk}=a_{il}a_{jm}a_{kn}d^p_{lmn}, \tag{10}$$

where ϕ, θ, and ψ are the Euler angles and a_{ij} is the element of the Euler matrix a that describes the rotation defined by the Euler angles. A caution is necessary when comparing data from different sources since Euler angles are not uniquely defined in the literature. Here, ϕ describes the first counterclockwise rotation around the original x_3 axis, θ is the second counterclockwise rotation around the new x_1 axis and ψ is the third counterclockwise rotation around the new x_3 axis. The transform matrix a from the Euler angles is given by[24]

$$a=\begin{pmatrix}\cos\psi\cos\phi-\cos\theta\sin\psi\sin\phi & \cos\psi\sin\phi+\cos\theta\sin\psi\cos\phi & \sin\theta\sin\psi\\ -\sin\psi\cos\phi-\cos\theta\cos\psi\sin\phi & -\sin\psi\sin\phi+\cos\theta\cos\psi\cos\phi & \sin\theta\cos\psi\\ \sin\theta\sin\phi & -\sin\theta\cos\phi & \cos\theta\end{pmatrix}. \tag{11}$$

With Eqs. (10) and (11) one can calculate the orientation dependence of the piezoelectric coefficient.

III. TEMPERATURE DEPENDENCE OF PIEZOELECTRIC PROPERTIES

To calculate the piezoelectric properties of $KNbO_3$ crystals, we use the coefficients for an eighth-order free energy function determined previously.[25] The electrostrictive coefficients and elastic compliance constants are $Q_{11}=0.12\ \mathrm{m^4/C^2}$, $Q_{12}=-0.053\ \mathrm{m^4/C^2}$, and $Q_{44}=0.052\ \mathrm{m^4/C^2}$ and $s_{11}=4.6\times10^{-12}\ \mathrm{m^2/N}$, $s_{12}=-1.1\times10^{-12}\ \mathrm{m^2/N}$, and $s_{44}=11.1\times10^{-12}\ \mathrm{m^2/N}$, respectively.[15,26,27] The dielectric permittivity ε^p_{ij} is related to the dielectric susceptibility η^p_{ij} with $\varepsilon^p_{ij}=1+\eta^p_{ij}\approx\eta^p_{ij}$. The temperature dependence of dielectric susceptibility coefficients η^p_{ij} and piezoelectric coefficients d^p_{ij} of $KNbO_3$ crystals for all three ferroelectric phases in the cubic crystallographic coordinate system can be calculated by using Eqs. (3) and (5). By rotating coordinate system from the cubic crystallographic coordinate system, one can obtain η^p_{ij} and d^p_{ij} in the new coordinate system as shown in Figs. 1 and 2, respectively. The new coordinate axes are expressed by the original system are $[100]^t=[100]^c$, $[010]^t=[010]^c$, and $[001]^t=[001]^c$ for the tetragonal phase, $[100]^o=[100]^c$, $[010]^o=[01\bar{1}]^c$, and $[001]^o=[011]^c$ for the orthorhombic phase, and $[100]^r=[01\bar{1}]^c$, $[010]^r=[\bar{2}11]^c$, and $[001]^r=[111]^c$ for the rhombohedral phase, respectively.

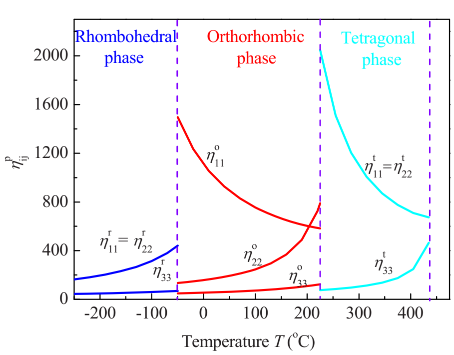

FIG. 1. (Color online) Calculated temperature dependence of the dielectric susceptibility coefficients η^p_{ij} for $KNbO_3$ single crystals in all three ferroelectric phases.

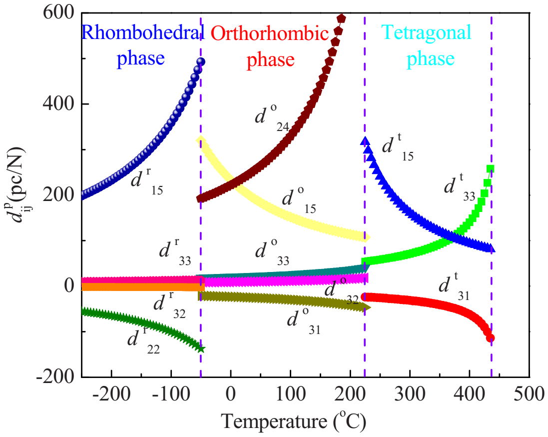

FIG. 2. (Color online) Calculated temperature dependence of piezoelectric coefficients d_{ij}^{p} for $KNbO_3$ single crystals in all three ferroelectric phases.

A. Tetragonal phase

In the tetragonal phase, the $KNbO_3$ crystal has $4mm$ symmetry. Since the coordinate system for the tetragonal phase is chosen as the same as the one in the cubic phase, $d_{ij}^{t}=d_{ij}^{c}$. After a rotation of angle θ with respect to the $[100]^t$, the longitudinal piezoelectric coefficient $d_{33}^{t*}(\theta)$ in the rotated coordinate can be expressed as

$$d_{33}^{t*}(\theta) = \cos\,\theta(d_{15}^{t}\sin^2\theta + d_{31}^{t}\sin^2\theta + d_{33}^{t}\cos^2\theta). \quad (12)$$

The Euler angle $\theta=45°$ is corresponding to the coordinates associated with the orthorhombic phase. We plot an orientation dependence of calculated $d_{33}^{t*}(\theta)$ of the tetragonal phase for three selected temperatures 230, 300, and 350 °C as shown in Fig. 3. It is shown that the surface of $d_{33}^{t*}(\theta)$ changes upon cooling from the Curie temperature. The direction of the largest $d_{33}^{t*}(\theta)$ is along $[001]_c$ direction at 350 °C then changes to $\theta_{max}=31.1°$ at 300 °C, and finally to $\theta_{max}=49.8°$ at 230 °C. Analyzing the expression of $d_{33}^{t*}(\theta)$, one can easily see that $d_{33}^{t*}(\theta)$ is determined by three parameters d_{33}^{t}, d_{31}^{t}, and d_{15}^{t}, which can be calculated by Eq. (6) (Fig. 2). It shows that d_{33}^{t} and d_{15}^{t} increase rapidly as the temperature approaches the tetragonal to cubic and tetragonal to orthorhombic phase transition temperatures while d_{31}^{t} only changes slightly in comparison with d_{33}^{t} and d_{15}^{t}. The increase in d_{15}^{t} with increasing temperature is similar to the behavior of the dielectric permittivity in the cubic phase, which increases when the crystal is cooled toward the ferroelectric phase.[28] From Eq. (6) it is easily seen that $d_{33}^{t}\propto\eta_{33}^{t}$ and $d_{15}^{t}\propto\eta_{11}^{t}$ or η_{22}^{t}, in which dielectric susceptibility is perpendicular to and parallel to the polar direction in the tetragonal phase, respectively. The calculated dielectric constants in the tetragonal phase are shown in Fig. 1, η_{11}^{t} and η_{33}^{t} exhibits opposite behaviors in the whole tetragonal phase temperature range. This leads to a maximum $d_{33\max}^{t*}(\theta)$ along the polar direction $[001]^c$ in the high-temperature range. As the temperature decreases toward the orthorhombic phase, the largest $d_{33\max}^{t*}(\theta)$ develops along a direction other than $[001]^t$. A plot of $d_{33}^{t*}(\theta)$ as a function of corresponding angle θ at several selected temperatures clearly shows the trend of maximum $d_{33\max}^{t*}(\theta)$ with temperature in Fig. 4. The maximum $d_{33\max}^{t*}(\theta)$ along $[001]^t$ direction can be expected at the high-temperature near the tetragonal-cubic transition point. As the temperature is lowered, d_{15}^{t} increases and $d_{33}^{t*}(\theta)$ gradually develops a local minimum along $[001]^t$ direction and then a global maximum at an angle away from $[001]^t$. Note that the largest $d_{33\max}^{t*}(\theta)$ still lies along $[001]^t$ ($\theta_{max}=0$) direction in the temperature range of tetragonal phase.

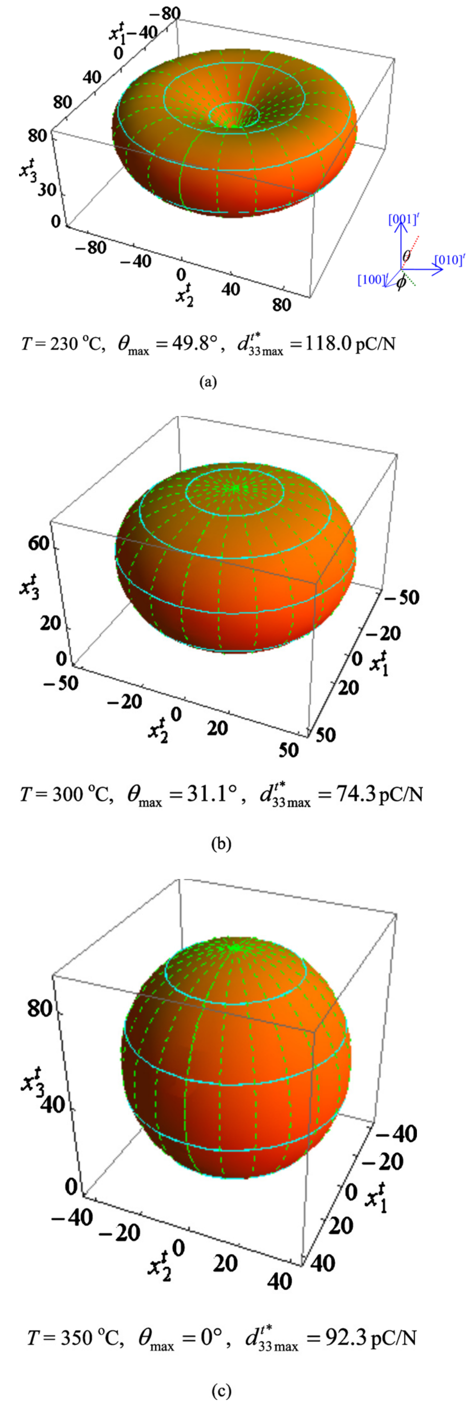

FIG. 3. (Color online) The orientation dependence of piezoelectric coefficients d_{33}^{t*} of $KNbO_3$ in the tetragonal phase for three selected different temperatures, (a) $T=230$ °C; (b) $T=300$ °C; and (c) $T=350$ °C. Angle θ_{max} at which maximum d_{33}^{t*} occurs is indicated for each temperature. Three coordinate axes correspond to $x_1^t=d_{33}^{t*}\sin\theta\cos\phi$, $x_2^t=d_{33}^{t*}\sin\theta\sin\phi$, and $x_3^t=d_{33}^{t*}\cos\theta$. The numerical values marked on the axes have unit pC/N. Only the upper half of the coordinate space is shown.

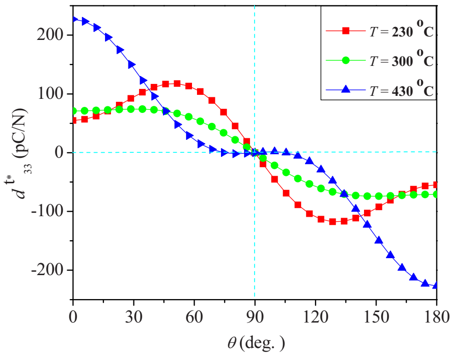

FIG. 4. (Color online) The piezoelectric coefficient d_{33}^{t*} in the tetragonal $KNbO_3$ as a function of angle θ at various temperatures.

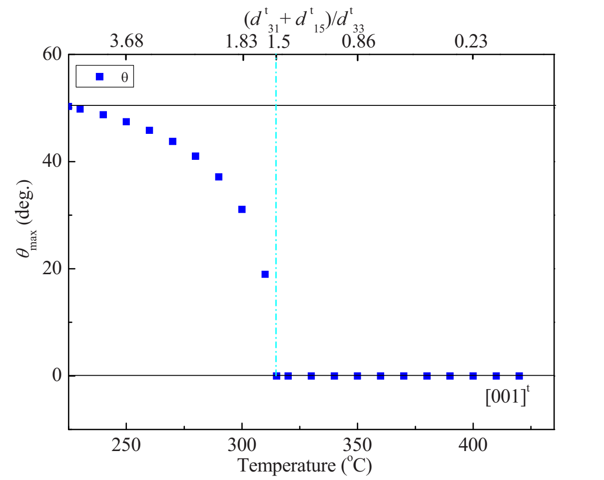

FIG. 5. (Color online) The angle θ_{max} indicating direction along which d_{33}^{t*} is the largest as a function of temperature and $(d_{31}^t + d_{15}^t)/d_{33}^t$ ratio.

For example, at the temperature $T=430$ °C, close to the cubic phase, the maximum $d_{33\max}^{t*}(\theta)=226.86$ pC/N is along the direction $[001]^c$, while at the temperature $T=230$ °C, close to the orthorhombic phase, the maximum $d_{33\max}^{t*}(\theta)=118.0$ pC/N is along the direction defined by $\theta_{max}=49.8°$. The maximum $d_{33\max}^{t*}(\theta)$ decreases with temperature above about 314 °C, and then increases below it. It is interesting to point out that it is different from other ferroelectric materials like $BaTiO_3$ (the maximum $d_{33\max}^{t*}(\theta)$ lies along the polar direction near to the tetragonal-cubic phase transition and has the largest value upon cooling of temperature with the direction along no-polar direction) and $PbTiO_3$ (the maximum $d_{33\max}^{t*}(\theta)$ always lies along the polar direction in the ferroelectric phase and the maximum closes to the tetragonal-cubic phase transition).[24] The angle θ_{max} for the maximum $d_{33\max}^{t*}(\theta)$ can be calculated by the relation of $\cos^2\theta_{max}=(d_{31}^t+d_{15}^t)/3(d_{31}^t+d_{15}^t-d_{33}^t)$, which is also plotted in Fig. 4. Damjanovic *et al.*[29] concluded that θ_{max} should satisfy a condition $0\leq\theta_{max}\leq 54.73°$ for all tetragonal perovskite materials. Our calculations show θ_{max} approaches 50.28° close to the orthorhombic phase. At the temperature below 314 °C, where $(d_{31}^t+d_{15}^t)/d_{33}^t \geq 1.5$, θ_{max} deviates from 0° (Fig. 5). The value of q $(q=3/2-Q_{12}/Q_{11})$ defined by Damjanovic[29] is calculated as 1.9. It is also easily shown that the maximum $d_{33\max}^{t*}(\theta)$ rotates from the polar direction once $q>1.9$ below 314 °C.

In the tetragonal phase, the significant increase in the dielectric susceptibility η_{11}^t or η_{22}^t along the $[100]^t$ or $[010]^t$ axes as the orthorhombic phase is approached upon cooling, which implies that the tetragonal $KNbO_3$ becomes dielectrically soft along crystallographic directions perpendicular to the polarization direction $[001]^t$. This case is predicted theoretically in materials exhibiting temperature driven ferroelectric-ferroelectric phase transitions.[21] $d_{33}^{t*}(\theta)$ is mainly determined by d_{15}^t close to the tetragonal-orthorhombic phase transition. For $KNbO_3$, although the polarization rotation effect is strong in this temperature range, it still does not dominate the piezoelectric response. In the high-temperature range approaching the cubic phase, d_{33}^t becomes dominant while d_{15}^t is relatively small. The enhanced d_{33}^t approaching the tetragonal-cubic phase transition can also be predicted form the flattening of the free energy profile [Fig. 6(a)].

B. Orthorhombic phase

In the orthorhombic phase, the temperature dependence of piezoelectric coefficient d_{33}^{o*} in $KNbO_3$ is more complex than the tetragonal phase. The orthorhombic phase has symmetry *mm*2 possessing two distinct different shear coefficients d_{15}^o and d_{24}^o. In order to study the orientation dependence of d_{33}^{o*} due to the phase transition, the Euler angles are chosen as $\psi=0$ and ϕ and θ varying arbitrarily. $\phi=\pi/2$ and $\theta=\arcsin(1/\sqrt{3})$ corresponds to the coordinate associated with the rhombohedral phase while $\phi=0$ and $\theta=\pi/4$ corresponds to the coordinate associated with the tetragonal phase. With such a coordinate transform, d_{33}^{o*} can be expressed by

$$d_{33}^{o*}(\phi,\theta) = \cos\theta[(d_{15}^o + d_{31}^o)\sin^2\theta\sin^2\phi + (d_{24}^o + d_{32}^o)\sin^2\theta\cos^2\phi + d_{33}^o\cos^2\theta]. \tag{13}$$

Since the transform matrix between the cubic and orthorhombic phase coordinate systems is

$$c_{ij} = \begin{pmatrix} 1 & 0 & 0 \\ 0 & \sqrt{2}/2 & -\sqrt{2}/2 \\ 0 & \sqrt{2}/2 & \sqrt{2}/2 \end{pmatrix}, \tag{14}$$

where the relation of piezoelectric constants in the two different coordinate systems can be expressed via Eqs. (7) and (9) as

$$d_{15}^o = \sqrt{2}d_{15O}^c,$$

$$d_{24}^o = \frac{2}{\sqrt{2}}(d_{33O}^c - d_{32O}^c),$$

$$d_{31}^o = \sqrt{2}d_{31O}^c,$$

$$d_{32}^o = \frac{1}{\sqrt{2}}(d_{33O}^c + d_{32O}^c - d_{24O}^c),$$

$$d_{33}^o = \frac{1}{\sqrt{2}}(d_{33O}^c + d_{32O}^c + d_{24O}^c),$$

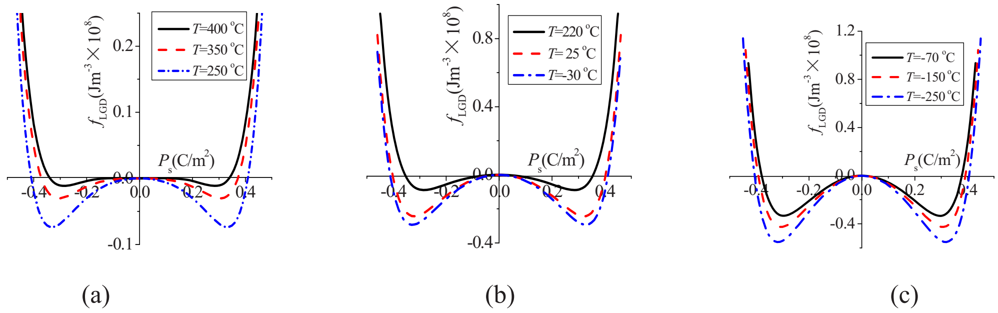

FIG. 6. (Color online) Calculated LGD-free energy as a function of polarizations (P_s) in all three ferroelectric phases at various selected temperatures.

$$d^o_{11} = d^o_{12} = d^o_{13} = d^o_{14} = d^o_{16} = d^o_{21} = d^o_{22} = d^o_{23} = d^o_{25} = d^o_{26} = d^o_{34} = d^o_{35} = d^o_{36} = 0. \tag{15}$$

By using $P^o_3 = \sqrt{2}P^c_{3O}$, $\eta^o_{11} = \eta^c_{11O}$, $\eta^o_{22} = \eta^c_{33O} - \eta^c_{23O}$, and $\eta^o_{33} = \eta^c_{33O} + \eta^c_{23O}$, one can get

$$d^o_{15} = \varepsilon_0 \eta^o_{11} Q_{44} P^o_3,$$

$$d^o_{24} = 2\varepsilon_0 \eta^o_{22}(Q_{11} - Q_{12})P^o_3,$$

$$d^o_{31} = 2\varepsilon_0 \eta^o_{33} Q_{12} P^o_3,$$

$$d^o_{32} = \frac{1}{2}\varepsilon_0 \eta^o_{33}(2Q_{11} + 2Q_{12} - Q_{44})P^o_3,$$

$$d^o_{33} = \frac{1}{2}\varepsilon_0 \eta^o_{33}(2Q_{11} + 2Q_{12} + Q_{44})P^o_3. \tag{16}$$

The temperature dependence of piezoelectric coefficients in $KNbO_3$ crystals in the orthorhombic phase is calculated with Eqs. (15) and (16) and is shown in Fig. 2. The shear piezoelectric coefficients d^o_{15} and d^o_{24} exhibit a strong temperature dependences and also have an opposite tendency, while other three components d^o_{31}, d^o_{32}, and d^o_{33} are relatively insensitive to temperature. Thus, the temperature dependence of d^{o*}_{33} is dominated by d^o_{15} and d^o_{24} as seen from Eq. (13). The piezoelectric constants at room temperature are given in Table I, which shows that the calculated d^o_{33}, d^o_{32}, and d^o_{31} agree well with previous results while d^o_{15} and d^o_{24} are slightly overestimated.

The three-dimension d^{o*}_{33} surfaces at three chosen temperatures -50, 25, and 220 °C are plotted in Fig. 7. The

TABLE I. Calculation obtained room temperature values of the piezoelectric coefficients, compared with previously published results.

Properties (pC/N)	Wada[a]	Zgonik[b]	Gunther[c]	Liang[d]	This work
d^o_{33}	29.6	29.3	24.5	27.4	21.6
d^o_{32}	18.5	9.8	9.8	3.4	9.5
d^o_{31}	−22.3	−19.5	−19.5	−24.3	−24.6
d^o_{15}	135.8	156.0	159.0	⋯	205.1
d^o_{24}	204.0	206.0	215.0	⋯	241.5

[a]Reference 7.
[b]Reference 16.
[c]Reference 15.
[d]Reference 27.

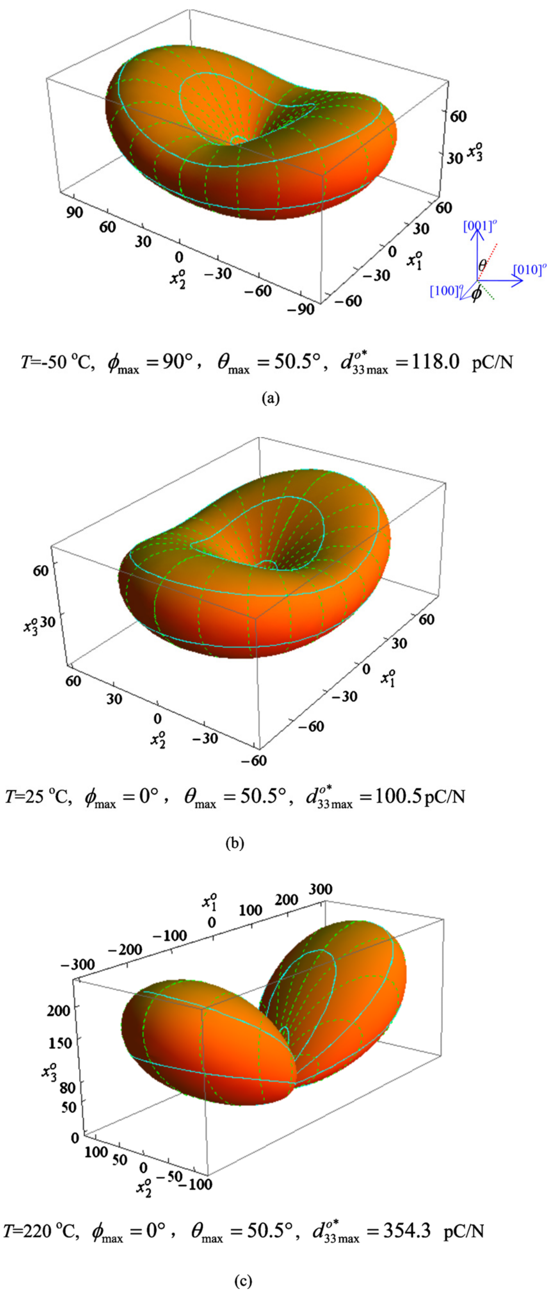

FIG. 7. (Color online) The orientation dependence of piezoelectric coefficients d^{o*}_{33} of $KNbO_3$ in the orthorhombic phase for three selected different temperatures, (a) $T=-50$ °C; (b) $T=25$ °C; and (c) $T=220$ °C. Angle θ_{max} at which maximum d^{o*}_{33} occurs is indicated for each temperature. The three coordinate axes correspond to $x^o_1 = d^{o*}_{33}\sin\theta\cos\phi$, $x^o_2 = d^{o*}_{33}\sin\theta\sin\phi$, and $x^o_3 = d^{o*}_{33}\cos\theta$. The numerical values marked on the axes have unit pC/N. Only the upper half of the coordinate space is shown.

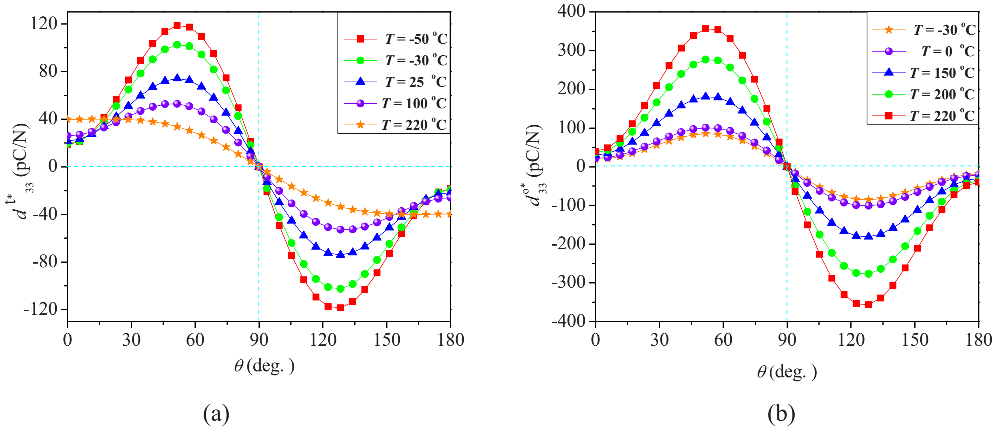

FIG. 8. (Color online) Piezoelectric coefficients d_{33}^{o*} in the orthorhombic $KNbO_3$ as a function of angle θ at various temperatures in different planes, (a) $\phi=90°$ and (b) $\phi=0°$.

maximum d_{33}^{o*} changes its direction upon cooling from the tetragonal-orthorhombic phase transition temperature. As a result, it leads to a rotation of maximum d_{33}^{o*} away from the polar direction $[001]^o$, which is attributed to the qualitatively opposite dependences of d_{15}^o and d_{24}^o on temperature. Approaching to the tetragonal-orthorhombic phase transition temperature, d_{24}^o dominates over d_{33}^{o*} [Eq. (13)], while d_{15}^o becomes dominant on cooling to the temperature near the orthorhombic-rhombohedral phase transition point. Different from the tetragonal phase, d_{33}^{o*} is dependent on two competitive shear piezoelectric coefficients in the orthorhombic phase.

In the orthorhombic phase, the two shear piezoelectric coefficients d_{15}^o and d_{24}^o are related to the permittivities perpendicular to the direction of the spontaneous polarization axis $[001]^o$. d_{15}^o is directly related to the presence of the orthorhombic-rhombohedral phase transition. The significant increase in the dielectric susceptibility η_{11}^o as the rhombohedral phase is approached on cooling implies that the orthorhombic $KNbO_3$ becomes dielectrically softened along the crystallographic direction perpendicular to the polarization direction $[001]^o$. The LGD-free energy well as a function of polarization shown in Fig. 6(b) becomes shallower with increasing temperature, leading to the increase in dielectric susceptibility, and thus the increase in its piezoelectric response. d_{24}^o is related to the tetragonal-orthorhombic phase transition and increases with increasing temperature. The increase in η_{22}^o close to the tetragonal phase can be reasonably explained by the rotation of polarization as the phase transition occurs. Therefore, d_{33}^{o*} in the orthorhombic phase is influenced by two adjacent ferroelectric phase transitions. The large longitudinal responses along no-polar directions are consistent with the results from first principle calculations, which interpreted the enhanced piezoelectric coefficients along no-polar directions by rotating the polarization induced by the strong external electric fields.[19,30] Its maximum as a function of angle depends on the competition of d_{15}^o and d_{24}^o. As shown in Fig. 2, d_{33}^{o*} is dominated by d_{15}^o close to the orthorhombic-rhombohedral phase transition temperature and by d_{24}^o close to the tetragonal-orthorhombic phase transition temperature. We analyze the values of d_{33}^{o*} on $(100)^o$ and $(010)^o$ assuming $\phi=0°$ and $\phi=90°$ and plot them as a function of angle θ under various temperatures in Fig. 8. On the $(010)^o$ plane with $\phi=90°$, the direction of maximum d_{33}^{o*} changes with decreasing temperature while it lies along the same direction as on the $(100)^o$ plane with $\phi=0°$. This can be easily seen from Fig. 9, in which the maximum $d_{33\max}^{o*}$ and its corresponding $\theta_{\max}$ are shown as a function of temperature. For $\phi=90°$, $d_{33\max}^{o*}$ increases with decreasing temperature and $\theta_{\max}$ increases rapidly and reaches 50.6° with decreasing temperature and then becomes independent of

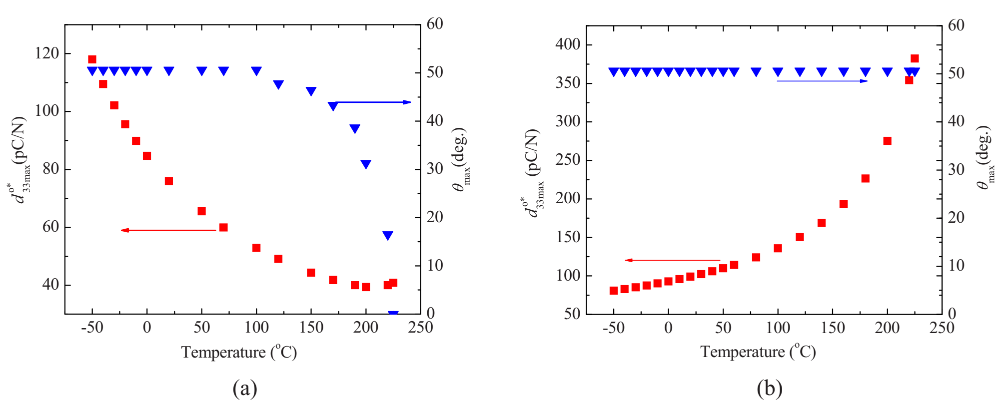

FIG. 9. (Color online) Maximum d_{33}^{o*} and its corresponding angle $\theta_{\max}$ as a function of temperature for the orthorhombic $KNbO_3$ in different planes, (a) $\phi=90°$ and (b) $\phi=0°$.

temperature below 100 °C. However, in the case of $\phi=0°$, $d^{o*}_{33\max}$ decreases with decrease in temperate and $\theta_{\max}$ remains constant. Our calculations show the surface of d^{o*}_{33} is nearly symmetrical on the $(100)°$ plane around −10 °C. The direction of the maximum $d^{o*}_{33\max}$ is rotated by 90° with increasing temperature.

The calculated results show that d^{o*}_{33} has the largest value in the high-temperature range approaching the tetragonal phase. This is different from $BaTiO_3$, in which it has the largest d^{o*}_{33} in the low temperature range close to the orthorhombic-rhombohedral phase transition. This also implies that the tetragonal-orthorhombic transition has stronger effects on the piezoelectric response than the orthorhombic-rhombohedral transition in $KNbO_3$.

At room temperature, the calculated $d^{o*}_{33\max}$ is nearly 100.5 pC/N with $\phi=0°$ and $\theta_{\max}=50.6°$. This is quantitatively consistent with the Nakamura's measurement results[11] which show the highest piezoelectric coefficient 92 pC/N through evaluating the strain versus electric field curve for the 49.5°-rotated $[100]^o$-cut about the $[010]^o$-axis of single-domain $KNbO_3$. However, based on our calculation results, there should exit another maximum d^{o*}_{33} with $\phi=90°$ and $\theta_{\max}=50.6°$.

C. Rhombohedral phase

For the low temperature rhombohedral phase, the orientation dependence of d^{r*}_{33} is given by

$$d^{r*}_{33}(\theta,\psi) = d^r_{15}\cos\theta\sin^2\theta - d^r_{22}\sin^3\theta + d^r_{31}\sin^2\theta\cos\theta + d^r_{33}\cos^3\theta. \tag{17}$$

Among the three Euler angles, $\phi=0°$ is fixed for simplicity. The rest two angles θ and ψ are varied to investigate the transition from rhombohedral to orthorhombic phase. $\theta=\arctan(-1/\sqrt{2})$ and $\psi=-\pi/2$ gives the coordinates associated with the orthorhombic phase.

The transform matrix between the cubic and rhombohedral phase coordinate systems is

$$c_{ij} = \begin{pmatrix} 0 & \sqrt{2}/2 & -\sqrt{2}/2 \\ -2/\sqrt{6} & 1/\sqrt{6} & 1/\sqrt{6} \\ 1/\sqrt{3} & 1/\sqrt{3} & 1/\sqrt{3} \end{pmatrix}. \tag{18}$$

Thus the relationship of the piezoelectric constants between two reference systems of the rhombohedral phase is given as

$$d^r_{15} = d^r_{24} = \frac{2d^c_{33R} - 2d^c_{32R} + d^c_{35R} - d^c_{36R}}{\sqrt{3}},$$

$$d^r_{16} = 2d^r_{21} = -2d^r_{22} = \sqrt{\frac{2}{3}}(d^c_{33R} - d^c_{32R} + d^c_{36R} - d^c_{35R}),$$

$$d^r_{31} = d^r_{32} = \frac{d^c_{33R} + 2d^c_{32R} - d^c_{35R} - d^c_{36R}/2}{\sqrt{3}},$$

$$d^r_{33} = \frac{d^c_{33R} + 2d^c_{32R} + 2d^c_{35R} + d^c_{36R}}{\sqrt{3}},$$

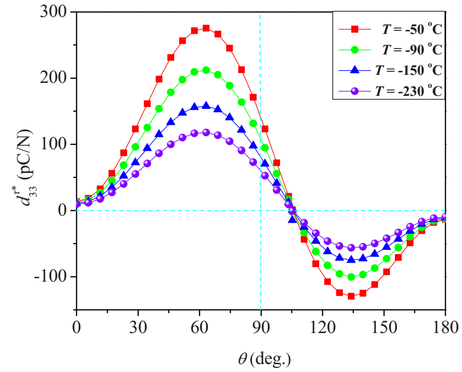

FIG. 10. (Color online) Piezoelectric coefficients d^{r*}_{33} in the orthorhombic $KNbO_3$ as a function of angle θ at various temperatures.

$$d^r_{11} = d^r_{12} = d^r_{13} = d^r_{14} = d^r_{23} = d^r_{25} = d^r_{26} = d^r_{34} = d^r_{35} = d^r_{36} = 0. \tag{19}$$

All piezoelectric constants can also be expressed as functions of the dielectric constants and polarizations by

$$d^r_{15} = d^r_{24} = \frac{1}{3}[4(Q_{11} - Q_{12}) + Q_{44}]\varepsilon_0\eta^r_{11}P^r_3,$$

$$d^r_{16} = 2d^r_{21} = -2d^r_{22} = \frac{\sqrt{2}}{3}(2Q_{11} - 2Q_{12} - Q_{44})\varepsilon_0\eta^r_{11}P^r_3,$$

$$d^r_{31} = d^r_{32} = \frac{1}{3}(2Q_{11} + 4Q_{12} - Q_{44})\varepsilon_0\eta^r_{33}P^r_3,$$

$$d^r_{33} = \frac{2}{3}[Q_{11} + 2Q_{12} + Q_{44}]\varepsilon_0\eta^r_{33}P^r_3, \tag{20}$$

where the relation of polarizations and dielectric susceptibilities, $P^r_3=\sqrt{3}P^c_{3R}$, $\eta^r_{11}=\eta^r_{22}=\eta^c_{11R}-\eta^c_{12R}$, and $\eta^r_{33}=\eta^c_{11R}+2\eta^c_{12R}$, between the two coordinate systems are used for calculations.

The calculated temperature dependence of d^r_{15}, d^r_{22}, d^r_{32}, and d^r_{33} are given in Fig. 2. d^r_{15} and d^r_{22} (negative value) increase with increasing temperature while d^r_{32} and d^r_{33} change slightly. Due to the absence of phase transitions in the lower temperature regime, the shear piezoelectric coefficient tensors are relatively to temperature around 0 K. The calculated three-dimensional surfaces of d^{r*}_{33} in the rhombohedral phase at three selected temperatures −70, −150, and −250 °C are nearly independent of temperature and the maximum $d^{r*}_{33\max}$ is reduced with decreasing temperature. For example, at −70 °C, $d^{r*}_{33\max}=239.8$ pC/N for $\theta_{\max}=61.8°$, while for −150 °C, $d^{r*}_{33\max}=158.0$ pC/N for $\theta_{\max}=61.7$ °C. $d^{r*}_{33\max}$ decreases into 110.9 pC/N for $\theta_{\max}=61.6°$ at −250 °C.

The piezoelectric coefficient d^{r*}_{33} in the rhombohedral $KNbO_3$ is plotted as a function of θ under various temperatures in Fig. 10. d^{r*}_{33} exhibits no-symmetry with respect to the axis defined by $\theta=90°$. This can be easily seen from the expression of d^{r*}_{33} [Eq. (17)], which includes a term $\sim d^o_{22}\sin^3\theta$. The no-zero term $\sim d^o_{22}\sin^3\theta$ at $\theta=90°$ gives different d^{r*}_{33} values in Fig. 10.

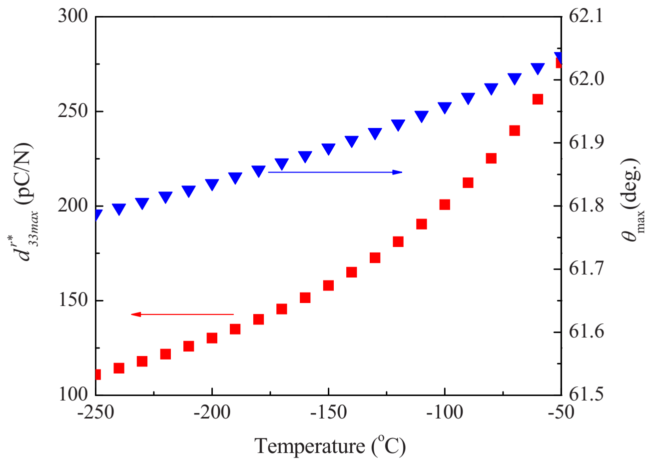

FIG. 11. (Color online) Maximum $d^{r*}_{33\max}$ and its corresponding angle $\theta_{\max}$ are as a function of temperature for the rhombohedral $KNbO_3$.

The maximum $d^{r*}_{33\max}$ and its corresponding angle $\theta_{\max}$ as a function of temperature are given in Fig. 11. $d^{r*}_{33\max}$ and $\theta_{\max}$ decrease with decreasing temperature. The angle $\theta_{\max}$ corresponding to the maximum d^{r*}_{33} is nearly independent of temperature.

From Eq. (20), d^{r}_{15} is determined by the dielectric susceptibility η^{r}_{11} (η^{r}_{22}), i.e., by the polarizability of a crystal perpendicular to the polarization direction, while d^{r}_{33} is controlled by the dielectric susceptibility η^{r}_{33} along the polar direction. As discussed above, the enhanced dielectric susceptibility is perpendicular to the polar direction and thus the enhanced piezoelectric response can be attributed to the rotation of polarization close to the phase transition. This leads to the increase in d^{r}_{15} with temperature approaching the orthorhombic phase. Therefore, d^{r*}_{33} is only affected by the rotation of polarization caused by the orthorhombic-rhombohedral phase transition. The flattening of the free energy well [Fig. 6(c)] also implies that the enhancement of piezoelectric coefficients is along a no-polar direction. The behavior of d^{r*}_{33} in the rhombohedral $KNbO_3$ is very similar to that in $BaTiO_3$.[21]

IV. CONCLUSIONS

The piezoelectric coefficient tensors and the orientation dependence of longitudinal piezoelectric coefficient d^{*}_{33} in $KNbO_3$ single crystals at different temperatures are analyzed using the LGD thermodynamic theory. The dielectric softening along the direction perpendicular to the polar direction is shown to be the main factor that contributes to the temperature dependence of the direction for the maximum d^{*}_{33}. Shear piezoelectric coefficients increase due to ferroelectric phase transitions leads to a significantly enhanced d^{*}_{33} along nonpolar directions. Similar behavior can be expected with respect to phase transitions caused by chemical composition variation, external electric field and mechanical pressure.

ACKNOWLEDGMENTS

The work is partially supported by NSF under Grant No. ECCS-0708759 and DMR-0507146.

[1]B. Jaffe, R. S. Roth, and S. Marzullo, J. Appl. Phys. **25**, 809 (1954).
[2]H. Jaffe, J. Am. Ceram. Soc. **41**, 494 (1958).
[3]Y. Hiruma, H. Nagata, and T. Takenaka, Jpn. J. Appl. Phys., Part 1 **45**, 7409 (2006).
[4]K. Yoshii, Y. Hiruma, H. Nagata, and T. Takenaka, Jpn. J. Appl. Phys., Part 1 **45**, 4493 (2006).
[5]K. Matsumoto, Y. Hiruma, H. Nagata, and T. Takenaka, Jpn. J. Appl. Phys., Part 1 **45**, 4479 (2006).
[6]E. Hollenstein, M. Davis, D. Damjanovic, and N. Setter, Appl. Phys. Lett. **87**, 182905 (2005).
[7]S. Wada, K. Muraoka, H. Kakemoto, T. Tsurumi, and H. Kumagai, Jpn. J. Appl. Phys., Part 1 **43**, 6692 (2004).
[8]S. E. Park and T. R. Shrout, J. Appl. Phys. **82**, 1804 (1997).
[9]S. Wada, S. Suzuki, T. Noma, T. Suzuki, M. Osada, M. Kakihana, S.-E. Park, L. E. Cross, and T. R. Shrout, Jpn. J. Appl. Phys., Part 1 **38**, 5505 (1999).
[10]S.-E. Park, S. Wada, L. E. Cross, and T. R. Shrout, J. Appl. Phys. **86**, 2746 (1999).
[11]K. Nakamura, T. Tokiwa, and Y. Kawamura, J. Appl. Phys. **91**, 9272 (2002).
[12]S. Wada, A. Seike, and T. Tsurumi, Jpn. J. Appl. Phys., Part 1 **40**, 5690 (2001).
[13]S. Saitoh, T. Kobayashi, K. Harada, S. Shimanuki, and Y. Yamashita, Jpn. J. Appl. Phys., Part 1 **37**, 3053 (1998).
[14]E. Wiesendanger, Ferroelectrics **6**, 263 (1974).
[15]P. Günter, Jpn. J. Appl. Phys., Part 1 **16**, 1727 (1977).
[16]M. Zgonik, R. Schlesser, I. Biaggio, E. Voit, J. Tscherry, and P. Gunter, J. Appl. Phys. **74**, 1287 (1993).
[17]R. Ahluwalia, T. Lookman, A. Saxena, and W. Cao, Phys. Rev. B **72**, 014112 (2005).
[18]L. Bellaiche, A. Garcıa, and D. Vanderbilt, Phys. Rev. B **64**, 060103 (2001).
[19]M. Budimir, D. Damjanovic, and N. Setter, Phys. Rev. B **72**, 064107 (2005).
[20]M. Budimir, D. Damjanovic, and N. Setter, Phys. Rev. B **73**, 174106 (2006).
[21]M. Budimir, D. Damjanovic, and N. Setter, J. Appl. Phys. **94**, 6753 (2003).
[22]M. J. Haun, E. Furman, S. J. Jang, and L. E. Cross, Ferroelectrics **99**, 13 (1989).
[23]J. F. Nye, *Physical Properties of Crystals* (Oxford Science Publications, New York, 1985).
[24]D. Damjanovic, M. Budimir, M. Davis, and N. Setter, J. Mater. Sci. **41**, 65 (2006).
[25]L. Liang, Y. L. Li, L.-Q. Chen, S. Y. Hu, and G.-H. Lu, Appl. Phys. Lett. **94**, 072904 (2009).
[26]L. E. Cross and G. A. Rossetti, J. Appl. Phys. **69**, 896 (1991).
[27]L. Liang, Y. L. Li, L.-Q. Chen, S. Y. Hu, and G.-H. Lu, J. Appl. Phys. **106**, 104118 (2009).
[28]M. Budimir, D. Damjanovic, and N. Setter, Appl. Phys. Lett. **85**, 2890 (2004).
[29]D. Damjanovic, F. Brem, and N. Setter, Appl. Phys. Lett. **80**, 652 (2002).
[30]H. Fu and R. E. Cohen, Nature (London) **403**, 281 (2000).